Frequency-domain and stochastic model for an articulated wave power device

J. Cândido[1] and P.A.P. Justino[2]

Department of Renewable Energies, Instituto Nacional de Engenharia, Tecnologia e Inovação
Estrada do Paço do Lumiar, 1649-038 Lisboa, Portugal
E-mail[1]: jose.candido@ineti.pt
E-mail[2]: paulo.justino@ineti.pt

Abstract

To have the first look into device performance, analytical and numerical tools must be used. Assuming that the wave power system hydrodynamics has a linear behaviour, diffraction and radiation coefficients can be computed. If the power take-off equipment may be, for the first approach, regarded as holding a linear behaviour then overall (i.e. hydrodynamic plus mechanical) device performance can be studied for regular waves. In this study a frequency-domain model describes the articulated system behaviour for regular waves.

For this paper a stochastic model is found for an articulated wave power device, and probability density functions are defined for the relevant parameters that characterize the wave power system behaviour. For these parameters and for different sea states the probability density functions are found. The articulated system is characterized by these probability density functions. Also, average values for capture width are obtained for these sea state conditions.

Keywords: Wave energy, frequency-domain, stochastic model.

Nomenclature

A_{ij} = added mass hydrodynamic coefficient
$\hat{A}$ = complex wave elevation amplitude
$\hat{A}_n$ = complex random amplitude
B_{ij} = damping hydrodynamic coefficient
C_i = hydrostatic restoring coefficient for body *i*
D_{L} = damping coefficient of the power take-off equipment
$E\{\ \}$ = expected value of
F_{D_i} = complex amplitude for the diffraction force on body *i*
F_{L} = load force
HG_1, HG_2 = transfer function
H_{s} = significant wave height
K_{L} = spring coefficient of the power take-off equipment
M_i = mass of body *i*
$\overline{P}_I$ = incident power for a regular wave
$\overline{P}_u$ = average useful power
S_η = spectral density
T = time interval
T_{e} = wave energy period
Z_{L} = load impedance
g = acceleration of gravity
h = water depth
k = wave number
t = time
φ_n = random phase
η = sea surface elevation
λ_c = capture width
θ = wave direction angle
ρ = water specific mass
σ^2 = variance
$\hat{\xi}_i$ = complex amplitude displacement for body *i*
$*$ = complex conjugate

Introduction

Since the beginning of the 20th century man has been thinking on how to make use of wave power. So far more than about thousands of patents have been registered. To have the first look into device performance, analytical and numerical tools must be used. Assuming that the wave power system hydrodynamics has a linear behaviour, diffraction and radiation coefficients can be computed using, for example, WAMIT© or Aquadyn. If the power take-off equipment can be, in the first approach, regarded as holding a linear behaviour, then overall (i.e. hydrodynamic plus mechanical) device performance can be studied for regular waves. In this study a frequency-domain

model describes the behaviour for regular waves of an articulated system consisting of two main concentric bodies. Optimal mechanical damping and spring coefficients are computed for some parameters (relative and absolute displacements) restrictions. Useful power, capture width, and other variables, like relative displacements (displacement of one body for a coordinate reference system that oscillates with the same amplitude and phase as the other body, i.e. a coordinate reference system fixed with respect to the second body), are computed for regular waves and the mechanical coefficients mentioned above. In [1] a theory for wave power absorption by two independently oscillating bodies has already been devised. Frequency analysis has been used to study devices such as Searev wave energy converter, [2], and also the hydrodynamic performance of arrays of devices as in [3]. As mentioned before software using panel methods can be used to compute the hydrodynamic coefficients of the two concentric bodies. In [4] hydrodynamic coefficients in heave of two concentric surface-piercing truncated circular cylinders were already computed.

A stochastic model has already been developed for OWC power plants [5]. This stochastic model has been used for optimization procedures of the FOZ do Douro OWC plant, [6], [7]. In this paper a stochastic model is found for the articulated wave power device, and probability density functions are defined for the relevant parameters that characterize the wave power system behaviour. Assuming that the overall system behaviour is linear and that the wave elevation for the irregular waves may be regarded as a stochastic process with a Gaussian probability density function, the variables that define the system behaviour, like, for example, displacements for the articulated system elements, will also have a Gaussian probability density function. For these parameters and for different sea states the probability density functions (i.e. variances) are found. The articulated system is characterized by these functions. Also, average values for capture width are obtained for these sea state conditions.

1 Mathematical models

The wave energy device is made of two concentric axisymmetric oscillating bodies, Fig. 1. The relative heave motion between bodies allows extracting power from sea waves. As usual it is assumed that the bodies have linear hydrodynamic behaviour and also that the power take-off can be modelled by spring and damping terms proportional to the relative displacement between bodies and to the relative velocity, respectively. A frequency domain model and a stochastic model are subsequently presented.

Frequency domain model

Applying Newton's second law, the governing equations for the wave energy device are,

$$-M_1\omega^2\bar{\xi}_1 = (\omega^2 A_{11} - i\omega B_{11})\bar{\xi}_1 + (\omega^2 A_{12} - i\omega B_{12})\hat{\xi}_2 + F_{D_1} - \\ - C_1\bar{\xi}_1 - (K_L + i\omega D_L)(\bar{\xi}_1 - \bar{\xi}_2), \tag{1}$$

and,

$$-M_2\omega^2\bar{\xi}_2 = (\omega^2 A_{22} - i\omega B_{22})\bar{\xi}_2 + (\omega^2 A_{21} - i\omega B_{21})\hat{\xi}_1 + F_{D_2} - \\ - C_2\bar{\xi}_2 + (K_L + i\omega D_L)(\bar{\xi}_1 - \bar{\xi}_2), \tag{2}$$

where ω is the angular frequency, $\bar{\xi}_i$ is the complex amplitude displacement for body i, M_i the mass of body i, C_i the hydrostatic restoring coefficient for body i, A_{ij} and B_{ij} the added mass and damping hydrodynamic coefficients, F_{D_i} the complex amplitude for the diffraction force on body i, and K_L and D_L the spring and damping coefficients of the power take-off equipment.

As given in [8] for the angular frequency ω the average useful power can be given by,

$$\overline{P}_u = \frac{1}{2} D_L \omega^2 \left|\hat{\xi}_1 - \hat{\xi}_2\right|^2. \tag{3}$$

Thus, choosing values for K_L and D_L it is possible to compute for each angular frequency and wave elevation amplitude the heave motions of the two concentric floating bodies, $\bar{\xi}_1$ and $\hat{\xi}_2$, as well as the average useful power, $\overline{P}_u$. The capture width, λ_c, may be computed by,

$$\lambda_c = \frac{\overline{P}_u}{\overline{P}_I} = \frac{2D_L\omega^3\left|\hat{\xi}_1 - \hat{\xi}_2\right|}{\rho g^2 \left|\hat{A}(\omega)\right|^2 \left(1 + \frac{2kh}{\sinh(2kh)}\right)\tanh(kh)}, \tag{4}$$

where $\overline{P}_I$ is the incident power for a regular wave with angular frequency ω and complex wave elevation amplitude $\hat{A}(\omega)$. The water depth is h, k is the wave number given by the positive root of the dispersion relationship, $\omega^2/g = k\tanh(kh)$, ρ is the water specific mass and g the acceleration of gravity.

Stochastic model

As in [5] we will consider a time interval of duration T, and assume that the sea surface elevation, $\eta(t)$, is a Gaussian random variable given by,

$$\eta(t) = \sum_{n=-\infty}^{+\infty} \hat{A}_n \exp(in\omega_0 t), \tag{5}$$

where $\omega_0 = 2\pi/T$, $\hat{A}_n = \left|\hat{A}_n\right|\exp(i\varphi_n)$ is a complex random variable with φ_n being a random variable uniformly distributed in the interval $[0;2\pi[$ and assuming that $E\left\{\left|\hat{A}_n\right|^2\right\} = \sigma_n^2$ and $E\left\{\hat{A}_n \hat{A}_{n'}^*\right\} = 0$, for $n \neq n'$.

Following [5] we find for the variance of the sea surface elevation, assuming that the sea state can be represented by a discrete power spectrum,

$$\sigma_\eta^2 = E\{\eta\eta^*\} = \sum_{n=-\infty}^{+\infty}\sum_{n'=-\infty}^{+\infty} \exp(i(n-n')\omega_0 t)\, E\{\hat{A}_n \hat{A}_{n'}^*\} = \\ = \sum_{n=-\infty}^{+\infty} \sigma_n^2. \tag{6}$$

As it is well known, if the sea surface power spectrum is continuous the variance of the elevation is given by

$$\sigma_\eta^2 = \int_{-\infty}^{+\infty} S_\eta(\omega) d\omega, \tag{7}$$

where $S_\eta(\omega)$ is a spectral density defined in the range $]-\infty;+\infty[$. Thus in the limiting case when $T \to \infty$ we will get $\omega_0 \to d\omega$ and $E\left\{\left|\hat{A}_n\right|^2\right\} = \sigma_n^2 \to S_\eta(\omega) d\omega$.

If the power spectrum is dependent not only on the wave frequency but also on the direction of the incoming waves we get for (5)

$$\eta(t) = \sum_{m=1}^{M}\sum_{n=-\infty}^{+\infty} \hat{A}_{nm} \exp(in\omega_0 t), \tag{8}$$

where M is the number of considered directions for the interval $[0;2\pi[$, $E\left\{\left|\hat{A}_{nm}\right|^2\right\} = \sigma_{nm}^2$ and $E\{\hat{A}_{nm}\hat{A}_{n'm'}^*\} = 0$ for $n \neq n'$ and $m \neq m'$. The variance of the elevation for a continuous power spectrum is now

$$\sigma_\eta^2 = \int_0^{2\pi}\int_{-\infty}^{+\infty} S_\eta(\omega,\theta) d\omega d\theta. \tag{9}$$

Taking into consideration that the two oscillating bodies are axisymmetric and that their behaviour in the frequency domain can be described by eqs. (1) and (2), it is possible to find transfer functions, $HG_1(n\omega_0)$ and $HG_2(n\omega_0)$, that relate the amplitude of the incident wave $\hat{A}_n$ and the displacement amplitude for body 1 and 2,

$$\hat{\xi}_1(n\omega_0) = HG_1(n\omega_0)\hat{A}_n, \tag{10}$$

and,

$$\hat{\xi}_2(n\omega_0) = HG_2(n\omega_0)\hat{A}_n. \tag{11}$$

According to (5) the vertical displacements for bodies 1 and 2 are described by,

$$\xi_1(t) = \sum_{n=-\infty}^{+\infty} HG_1(n\omega_0)\hat{A}_n \exp(in\omega_0 t), \tag{12}$$

and

$$\xi_2(t) = \sum_{n=-\infty}^{+\infty} HG_2(n\omega_0)\hat{A}_n \exp(in\omega_0 t). \tag{13}$$

Note that just as η, also ξ_1 and ξ_2 are Gaussian random variables, with variances

$$\sigma_{\xi_1}^2 = E\{\xi_1\xi_1^*\} = \sum_{n=-\infty}^{+\infty} |HG_1(n\omega_0)|^2 \sigma_n^2, \tag{14}$$

and

$$\sigma_{\xi_2}^2 = E\{\xi_2\xi_2^*\} = \sum_{n=-\infty}^{+\infty} |HG_2(n\omega_0)|^2 \sigma_n^2. \tag{15}$$

If the sea state can be represented by a continuous power spectrum, then we get for ξ_1 and ξ_2 variances

$$\sigma_{\xi_1}^2 = \int_{-\infty}^{+\infty} S_\eta(\omega)|HG_1(\omega)|^2 d\omega, \tag{16}$$

and

$$\sigma_{\xi_2}^2 = \int_{-\infty}^{+\infty} S_\eta(\omega)|HG_2(\omega)|^2 d\omega. \tag{17}$$

It is straightforward that the variance for the velocity of bodies 1 and 2 may be computed by,

$$\sigma_{\dot{\xi}_1}^2 = \int_{-\infty}^{+\infty} S_\eta(\omega)\omega^2|HG_1(\omega)|^2 d\omega, \tag{18}$$

and

$$\sigma_{\dot{\xi}_2}^2 = \int_{-\infty}^{+\infty} S_\eta(\omega)\omega^2|HG_2(\omega)|^2 d\omega. \tag{19}$$

Assuming that the load force, F_L, can be given by

$$F_L(t) = \pm\sum_{n=-\infty}^{+\infty}(K_L + in\omega_0 D_L)\left(\hat{\xi}_1(n\omega_0) - \hat{\xi}_2(n\omega_0)\right)\exp(in\omega_0 t), \tag{20}$$

we get, for the variance of the load force,

$$\sigma_{F_L}^2 = E\{F_L F_L^*\} = \\ = \sum_{n=-\infty}^{+\infty}\sum_{n'=-\infty}^{+\infty} Z_L(n\omega_0)Z_L^*(n'\omega_0)E\left\{\left(\hat{\xi}_1 - \hat{\xi}_2\right)_n\left(\hat{\xi}_1 - \hat{\xi}_2\right)_{n'}^*\right\} \times \\ \times \exp(i(n-n')\omega_0 t), \tag{21}$$

with $Z_L(n\omega_0) = K_L + in\omega_0 D_L$.

Since ξ_1 and ξ_2 are given by eqs. (12-13) and $E\{(\hat{\xi}_1 - \hat{\xi}_2)_n(\hat{\xi}_1 - \hat{\xi}_2)_{n'}\} = 0$ for $n \neq n'$, we get for the variance of F_L

$$\sigma_{F_L}^2 = \sum_{n=-\infty}^{+\infty}|Z_L(n\omega_0)|^2|HG_1(n\omega_0) - HG_2(n\omega_0)|^2\sigma_n^2. \tag{22}$$

Thus, for a continuous power spectrum we may write

$$\sigma_{F_L}^2 = \int_{-\infty}^{+\infty} S_\eta(\omega)|Z_L(\omega)|^2|HG_1(\omega) - HG_2(\omega)|^2 d\omega. \tag{23}$$

The average useful power may be written as

$$\overline{P_u} = D_L E\left\{\left|\dot{\xi}_1(t) - \dot{\xi}_2(t)\right|^2\right\}, \tag{24}$$

taking into consideration that for a sea state represented by a continuous power spectrum we get

$$E\left\{\left|\dot{\xi}_1-\dot{\xi}_2\right|^2\right\}=E\left\{\left(\dot{\xi}_1-\dot{\xi}_2\right)\left(\dot{\xi}_1-\dot{\xi}_2\right)^*\right\}= \\ =\int_{-\infty}^{+\infty}S_\eta(\omega)\omega^2\left|HG_1(\omega)-HG_2(\omega)\right|^2 d\omega. \quad (25)$$

Note that the probability of the instantaneous useful power being less or equal than $\chi^2 D_{\mathrm{L}}$ is given by

$$\mathrm{Prob}\left(P_u\le\chi^2 D_{\mathrm{L}}\right)=\int_{-\chi}^{\chi}\exp\left(\frac{-x^2}{2E\left\{\left|\dot{\xi}_1-\dot{\xi}_2\right|^2\right\}}\right)dx. \quad (26)$$

2 Numerical results

To illustrate the application of the frequency-domain model and mainly the stochastic model, results were obtained for the oscillating body presented in Fig. 1. It is assumed that body 1 is the body with a toroidal shape (outside body) and body 2 is the inside body made of two parts (one surface-piercing body and a completely submerged cylinder) that oscillate together. WAMIT© was used to compute the hydrodynamic diffraction and radiation coefficients for a set of 102 wave frequencies in the range of 0.2119 rad/s to 1.2778 rad/s. The water depth is 50m.

Assuming two scenarios for the power take-off equipment: a) it can only be simulated by a damping, D_{L}, coefficient, b) it can be simulated by spring, K_{L}, and damping coefficients, values were computed for K_{L} and D_{L} that maximize the average useful power, $\overline{P}_u$, and thus the capture width, λ_c. Several restrictions were also imposed on the amplitude of the heave motion of body 1 and on the amplitude of the relative heave motion between body 1 and body 2, $\left|\xi_1-\xi_2\right|$, for an incident wave with amplitude of 1m.

For scenario a) the capture width, mechanical damping coefficient, relative amplitude displacement between bodies and absolute amplitude displacements are presented in Figs. 2 to 6, respectively. They are obtained for different displacement restrictions. In all the cases it is assumed that the amplitude for the relative displacement between body 1 and body 2 cannot exceed 5m for an incident wave of 1m amplitude. It is also considered that the absolute displacement amplitude for body 1 cannot exceed 4, 5, 6, 7 and 8m. Thus the case "5_6" means that the amplitude for the relative displacement cannot exceed 5m and the amplitude for the absolute displacement cannot be greater than 6m. It can be observed from Fig. 2 that the device has two well defined capture width peaks, one at 5.5s and another at 8.7s. The value for the average useful power for the second peak (at 8.7s) is closely related to the allowed maximum amplitude heave motion for the first body, Fig. 5. To be able to control this amplitude, appropriate mechanical damping coefficients need to be chosen, Fig. 3. Note that if there are restrictions on the relative displacement between bodies and on the absolute displacement of body 1 then there will be restrictions for the absolute displacement of body 2, implicitly.

For scenario b), Figs. 7 to 12 present capture width, mechanical damping and spring coefficients, relative amplitude displacement and absolute amplitude displacements, respectively. Again, in all the cases it is assumed that the amplitude for the relative displacement between body 1 and body 2 cannot exceed 5m and that the absolute displacement amplitude for body 2 cannot exceed 4, 5 and 8m. As expected, for different maximum amplitude displacements of body 1 we get different capture widths – for lower values for body 1 maximum absolute displacement amplitude we get smaller values for capture width – Fig. 7. Indeed, damping and spring coefficients must be tuned out to allow for the restrictions to be achieved, Figs. 8 and 9. It may be observed from Fig. 11 that the absolute displacement amplitude for body 1 is bounded, as well as the relative displacement amplitude between bodies, Fig. 10.

For the stochastic model results are shown for irregular waves. Again, the two scenarios for the power take-off equipment above explained were considered. The spring and damping coefficients that maximize eq. (24), and thus the respective capture width, $\overline{\lambda_c}$, were computed. Results are obtained for the variance of ξ_1 and ξ_2, as well as for the variance of the load force, F_{L}. The best K_{L} and D_{L} for each sea state are also shown. The variances for ξ_1, ξ_2 and F_{L} were obtained for sea states with H_{s}, the sea state significant wave height, equal to 2m. Knowing that $\sigma^2_{\xi_1}$, $\sigma^2_{\xi_2}$ and $\sigma^2_{F_{\mathrm{L}}}$ are given by eqs. (16), (17) and (23), respectively, it is easily found that the variances are proportional to the square of H_{s}, i.e., if we multiply H_{s} by 2, the variances will be multiplied by 4, assuming that T_{e}, the sea state wave energy period, is kept constant as well as K_{L} and D_{L}. To represent the sea states the following frequency spectrum was adopted ([9]):

$$S_\eta(\omega)=131.5H_{\mathrm{s}}^2T_{\mathrm{e}}^{-4}\omega^{-5}\exp\left(-1054T_{\mathrm{e}}^{-4}\omega^{-4}\right) \quad (27)$$

The device behaviour was simulated for wave energy periods from 7 to 10s and for a H_{s} equal to 2m. As already mentioned, two different scenarios were considered for the power take-off equipment. Figs. 13 to 18 present the capture width, mechanical damping, spring coefficient and variances for the displacements of body 1 and 2, and load force, for both power take-off scenarios, respectively. It can be observed that the system has a better performance for sea states with smaller wave energy period, Fig. 13. For the range of considered wave energy periods the damping coefficients for scenario a) are greater than the ones computed for scenario b), Fig. 14. The spring coefficients computed for scenario b) may be negative or positive,

depending on the wave energy period, Fig. 15. For scenario a) the curves for the displacement variance of both bodies are similar, Fig. 16. However, these curves are rather different for scenario b), Fig. 17. The variance for the load force converges for both scenarios when the wave energy period increases, Fig. 18. As the capture width is quite different for T_e equal to 7s for the considered scenarios, the variance for the load force should also be different as it is observed in Fig. 18. The obtained variances allow defining Gaussian probability density functions for the analyzed parameters.

3 Conclusions

Frequency-domain and stochastic models were devised for an articulated device composed by two concentric bodies. Results were obtained for regular and irregular waves. The use of the stochastic model for irregular waves allows to find variances that define Gaussian probability density functions for relevant wave device parameters. It was assumed that the power take-off mechanical equipment has a linear behaviour and can be modelled by spring and damping coefficients. For irregular waves it was assumed that the characteristics of the power take-off system are constant for the duration of a sea state. As expected, the capture widths for the stochastic model are significantly lower than the ones obtained for the frequency-domain model. In order to have better performances for irregular waves, device control will be essential.

References

[1] M.A. Srokosz and D.V. Evans. A theory for wave-power absorption by two independently oscillating bodies. *J. Fluid Mechanics*, 90(2):337-362, 1979.

[2] A. Clément, A. Babarit, J-C. Gilloteaux, C. Josset and G. Duclos. The *SEAREV* wave energy converter. In *Proc. 6th European Wave and Tidal Energy Conference*, Glasgow, 2005.

[3] P.A.P. Justino and A. Clément. Hydrodynamic performance for small arrays of submerged spheres. In *Proc. 5th European Wave Energy Conference*, Cork, 2003.

[4] S. Mavrakos. Hydrodynamic coefficients in heave of two concentric surface-piercing truncated circular cylinders. *Applied Ocean Research*, 26:84-97, 2004.

[5] A.F. de O. Falcão and R.J.A. Rodrigues. Stochastic modelling of OWC wave power plant performance. *Applied Ocean Research*, 24:59-71, 2002.

[6] L.M.C. Gato, P.A.P. Justino and A.F. de O. Falcão. Optimization of power take-off equipment for an oscillating-water column wave energy plant. *6th European Wave and Tidal Energy Conference*, Glasgow, 2005.

[7] M.T. Pontes, J. Cândido, J.C.C. Henriques and P. Justino. Optimizing OWC sitting in the nearshore. In *Proc. 6th European Wave and Tidal Energy Conference*, Glasgow, 2005.

[8] J. Falnes. *Ocean waves and oscillating systems*. Cambridge University Press 2002.

[9] Y. Goda. *Random Seas and Design of Maritime Structures*. University of Tokyo Press 1985.

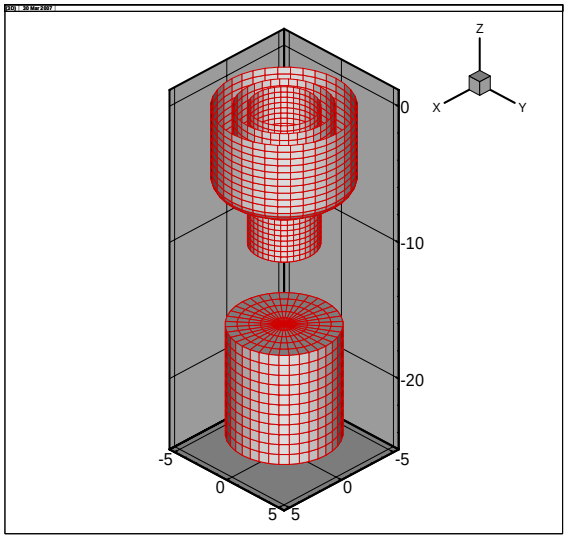

Figure 1: Panel grid describing the wet surface of the concentric axisymmetric oscillating bodies in numerical evaluation.

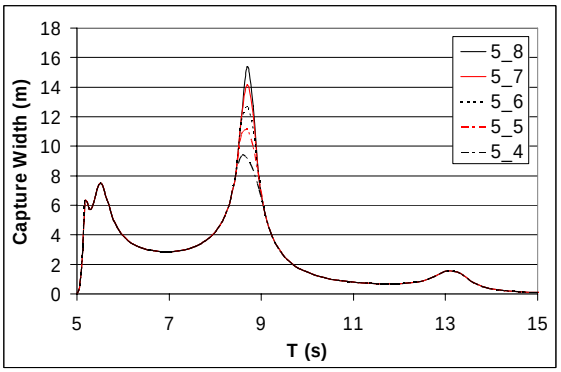

Figure 2: Capture width for a 5m maximum displacement amplitude between body 1 and body 2 (for an incident wave of 1m amplitude) and maximum absolute displacement amplitude for body 1 varying between 4m and 8m, assuming that the power take-off equipment can only be simulated by a damping coefficient D_L .

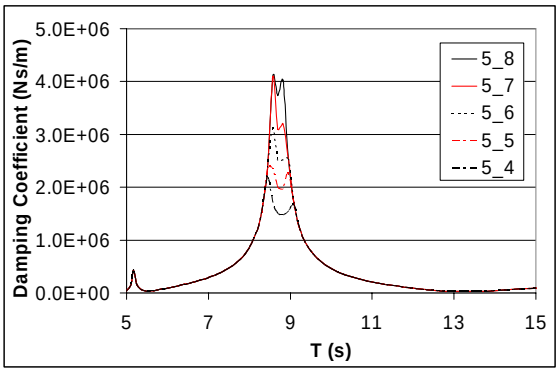

Figure 3: Mechanical damping coefficient for a 5m maximum displacement amplitude between body 1 and body 2 (for an incident wave of 1m amplitude) and maximum absolute displacement amplitude for body 1 varying between 4m and 8m, assuming that the power take-off equipment can only be simulated by a damping coefficient D_{L} .

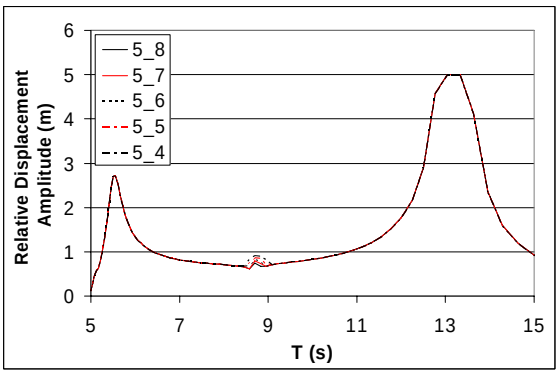

Figure 4: Relative displacement amplitude between body 1 and body 2 (for an incident wave of 1m amplitude) for maximum absolute displacement amplitude for body 1 varying between 4m and 8m, assuming that the power take-off equipment can only be simulated by a damping coefficient D_{L} .

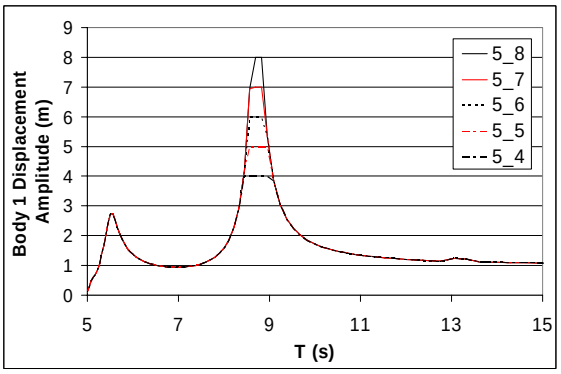

Figure 5: Absolute displacement amplitude for body 1 (for an incident wave of 1m amplitude), considering a 5m maximum displacement amplitude between body 1 and body 2, and an absolute displacement amplitude restriction varying between 4m and 8m, assuming that the power take-off equipment can only be simulated by a damping coefficient D_{L} .

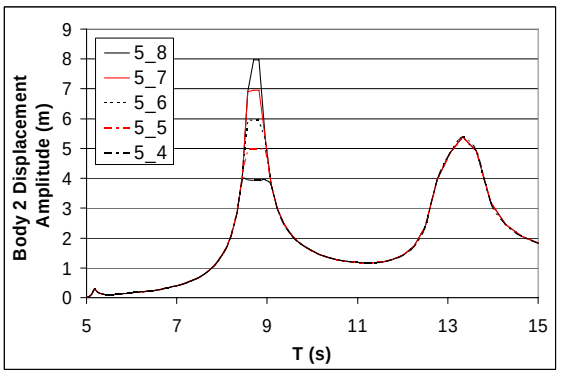

Figure 6: Absolute displacement amplitude for body 2 (for an incident wave of 1m amplitude), considering a 5m maximum displacement amplitude between body 1 and body 2, and an absolute displacement amplitude restriction for body 1 varying between 4m and 8m, assuming that the power take-off equipment can only be simulated by a damping coefficient D_{L} .

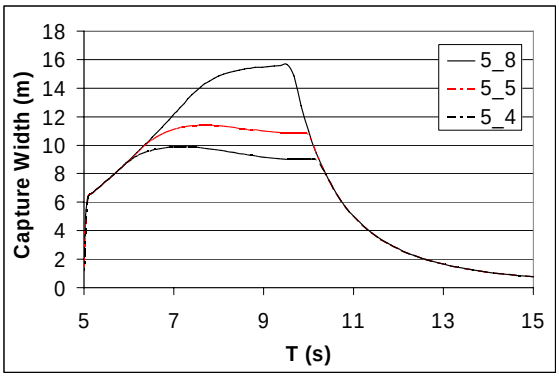

Figure 7: Capture width for a 5m maximum displacement amplitude between body 1 and body 2 (for an incident wave of 1m amplitude) and different maximum absolute displacement amplitudes for body 1 of 4m, 5m and 8m, assuming that the power take-off equipment can be simulated by damping and spring coefficients D_{L} and K_{L}.

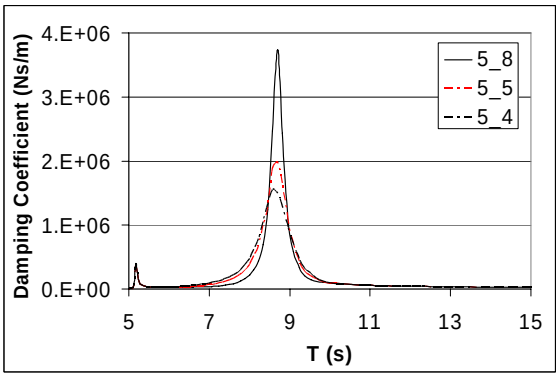

Figure 8: Mechanical damping coefficient for a 5m maximum displacement amplitude between body 1 and body 2 (for an incident wave of 1m amplitude) and different maximum absolute displacement amplitudes for body 1 of 4m, 5m and 8m, assuming that the power take-off equipment can be simulated by damping and spring coefficients D_{L} and K_{L}.

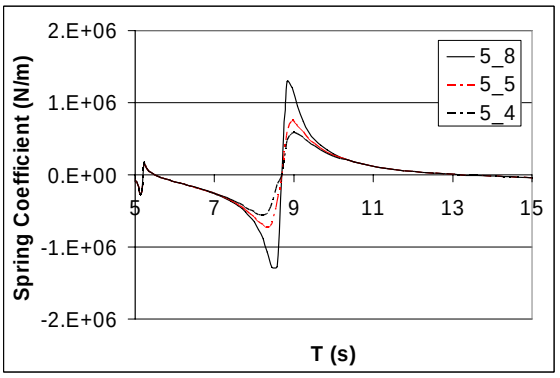

Figure 9: Mechanical spring coefficient for a 5m maximum displacement amplitude between body 1 and body 2 (for an incident wave of 1m amplitude) and different maximum absolute displacement amplitudes for body 1 of 4m, 5m and 8m, assuming that the power take-off equipment can be simulated by damping and spring coefficients D_{L} and K_{L}.

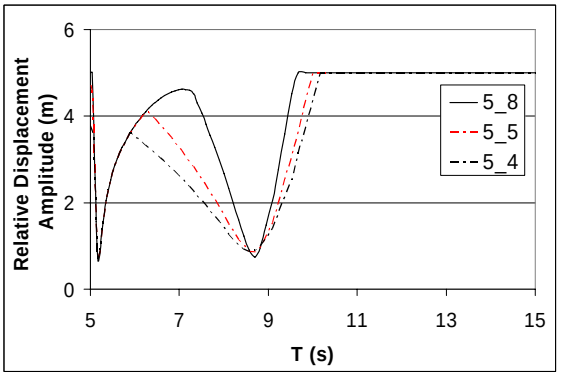

Figure 10: Relative displacement amplitude between body 1 and body 2 (for an incident wave of 1m amplitude) for different maximum absolute displacement amplitudes for body 1 of 4m, 5m and 8m, assuming that the power take-off equipment can be simulated by damping and spring coefficients D_{L} and K_{L}.

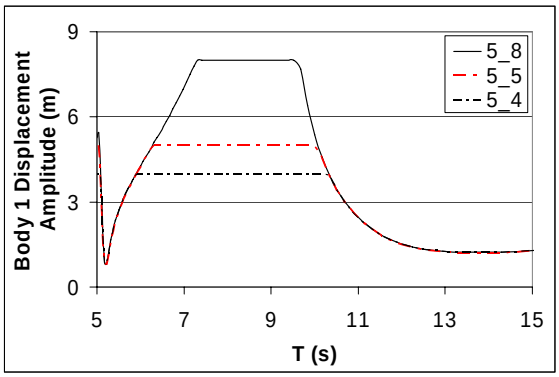

Figure 11: Absolute displacement amplitude for body 1 (for an incident wave of 1m amplitude), considering a 5m maximum displacement amplitude between body 1 and body 2, and absolute displacement amplitude restrictions of 4m, 5m and 8m, assuming that the power take-off equipment can be simulated by damping and spring coefficients D_L and K_L.

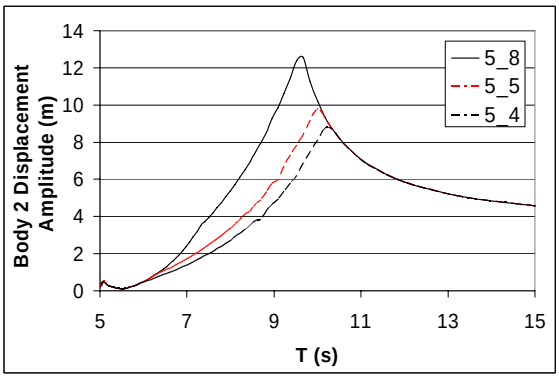

Figure 12: Absolute displacement amplitude for body 2 (for an incident wave of 1m amplitude), considering a 5m maximum displacement amplitude between body 1 and body 2, and absolute displacement amplitude restrictions for body 1 of 4m, 5m and 8m, assuming that the power take-off equipment can be simulated by damping and spring coefficients D_L and K_L.

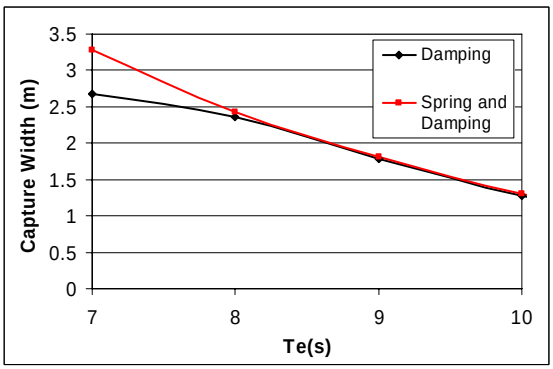

Figure 13: Capture width for wave energy periods from 7 to 10s and H_s equal to 2m, assuming that the power take-off equipment can only be simulated by a damping coefficient D_L (black line) and assuming that the power take-off equipment can be simulated by both damping and spring coefficients D_L and K_L (red line).

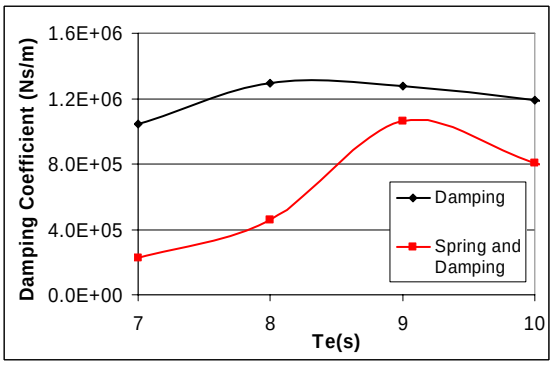

Figure 14: Mechanical damping coefficient for wave energy periods from 7 to 10s and H_s equal to 2m, assuming that the power take-off equipment can only be simulated by a damping coefficient D_L (black line) and assuming that the power take-off equipment can be simulated by both damping and spring coefficients D_L and K_L (red line).

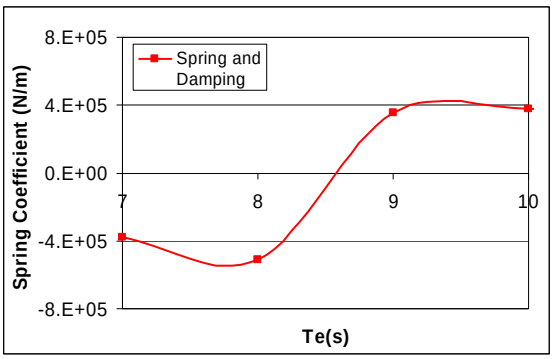

Figure 15: Mechanical spring coefficient for wave energy periods from 7 to 10s and H_s equal to 2m, assuming that the power take-off equipment can be simulated by both damping and spring coefficients D_L and K_L.

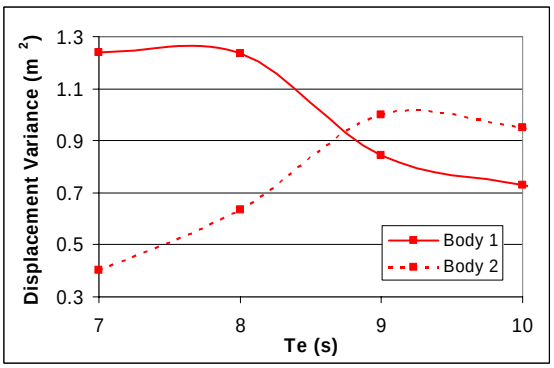

Figure 17: Variances for the displacements of body 1 and 2, for wave energy periods from 7 to 10s and H_s equal to 2m, assuming that the power take-off equipment can be simulated by both damping and spring coefficients D_L and K_L.

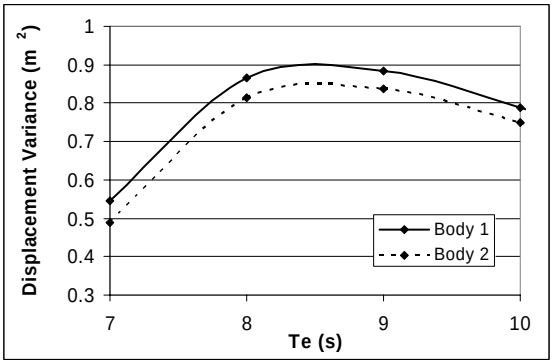

Figure 16: Variances for the displacements of body 1 and 2, for wave energy periods from 7 to 10s and H_s equal to 2m, assuming that the power take-off equipment can only be simulated by a damping coefficient.

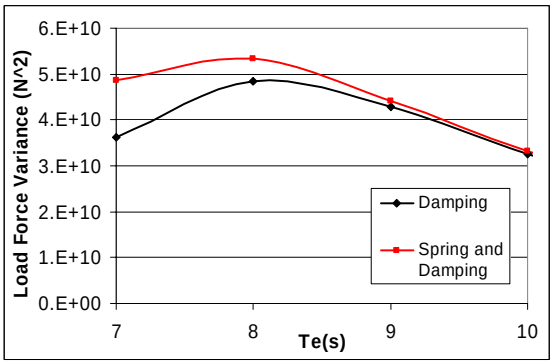

Figure 18: Variance for load force, for wave energy periods from 7 to 10s and H_s equal to 2m, assuming that the power take-off equipment can only be simulated by a damping coefficient D_L (black line) and assuming that the power take-off equipment can be simulated by both damping and spring coefficients D_L and K_L (red line).